# Combined optical and acoustic resolution photoacoustic microscopy

Moothanchery, Mohesh; Pramanik, Manojit

2017

Moothanchery, M., & Pramanik, M. (2017). Combined optical and acoustic resolution photoacoustic microscopy. Proceeding of SPIE 10064, Photons Plus Ultrasound: Imaging and Sensing 2017, 100644P-.

https://hdl.handle.net/10356/80361

https://doi.org/10.1117/12.2251258

# Combined optical and acoustic resolution photoacoustic microscopy

Mohesh Moothanchery and Manojit Pramanik*

School of Chemical and Biomedical Engineering, Nanyang Technological University, Singapore

## ABSTRACT

Photoacoustic imaging is a fast growing *in vivo* imaging modality combining the optical absorption contrast and high spatial ultrasonic resolution. Using this technique deeper tissue penetration greater than optical mean free path (~1 mm in skin) is possible. Low resolution with deep penetration depth is possible utilizing acoustic focusing and high resolution with shallow imaging depth can be possible by optical focusing using different photoacoustic microscopy (PAM) systems. Here, we present a combined/switchable optical resolution and acoustic resolution photoacoustic microscopy (OR-AR-PAM) system capable of both high resolution and low resolution deep tissue imaging on the same sample. Lateral resolution of 3.9 μm using optical focusing and lateral resolution of 57 μm using acoustic focusing was successfully demonstrated using the combined system.

**Keywords:** Photoacoustic Imaging, Optical resolution photoacoustic microscopy, Acoustic resolution photoacoustic microscopy, AR-PAM, AR-PAM.

## 1. INTRODUCTION

Photoacoustic microscopy (PAM) is an emerging hybrid *in vivo* imaging modality, combining optics and ultrasound which can provide deeper imaging than other optical modalities including multiphoton microscopy, confocal microscopy, and optical coherence tomography (OCT) where optical scattering in soft tissues degrades spatial resolution with imaging depth.[1-4] Combining strong optical absorption contrast and high ultrasound spatial resolution PAM can provide deeper imaging and has been successfully applied to *in vivo* imaging.[5-15] In PAM a short laser pulse will irradiate the sample/tissue. Tissue chromophores (such as melanin, red blood cells, water etc.) will absorb the light and will produce pressure waves, as a result of temperature rise these pressure waves are emitted in the form of acoustics waves [known as photoacoustic (PA) waves]. An ultrasonic transducer will receive the PA waves outside the sample/tissue boundary. In acoustic resolution photoacoustic microscopy (AR-PAM) utilizing weak optical and tight acoustic focusing lateral resolution of 45 μm and imaging depth up to 3 mm have been demonstrated[16] In optical resolution photoacoustic microscopy (OR-PAM), the lateral resolution can be improved by tight optical focus, and resolution up to 0.5 μm have been demonstrated.[17] Imaging depth image up to ~1.2 mm inside the biological tissue was reported using OR-PAM.[18]

Combining OR-PAM and AR-PAM will be of great benefit where high resolution and deeper imaging is needed. Not many efforts have been taken to combine both these systems together. In one approach an optical fiber bundle is used to delivery light for both OR and AR PAM. In this approach they have used two separate lasers (high energy for the AR and a low energy high repetition rate laser for the OR), making the system inconvenient and expensive.[19] In another approach for doing AR and OR PAM the optical and ultrasound focus has been shifted which makes the light focus and ultrasound focus not aligned, hence the image quality was not optimal.[20] Another approach of changing the optical fiber and collimating optics was reported makes the alignment process difficult.[21] In any of these cases ARPAM did not use a dark field illumination. Here, we report a switchable OR and AR PAM (OR-AR-PAM) imaging system capable of both high resolution imaging as well as low resolution deep tissue imaging on the same sample utilizing the same laser and scanner for both the system. The performance of the OR-AR-PAM system was characterized by determining spatial resolution, imaging depth using phantom experiments. *In vivo* blood vasculature imaging was performed on mouse ear for demonstrating its biological imaging capability.

* E-mail: manojit@ntu.edu.sg

Photons Plus Ultrasound: Imaging and Sensing 2017, edited by Alexander A. Oraevsky, Lihong V. Wang, Proc. of SPIE Vol. 10064, 100644P · © 2017 SPIE · CCC code: 1605-7422/17/$18 · doi: 10.1117/12.2251258

## 2. SYSTEM DESCRIPTION

The schematic of the OR-AR-PAM system is shown in Fig. 1.[22,23] This OR-AR-PAM system employs a nanosecond tunable laser system, consist of a diode-pumped solid-state Nd-YAG laser (INNOSLAB, Edgewave) and a dye laser (Credo-DYE-N, Sirah dye laser, Spectra physics). For AR-PAM scanning the laser beam was diverted using right angle prisms, RAP1 was placed on a computer controlled motorized stage (CR1/M-Z7, Thorlabs). The diverted beam passed through a variable neutral density filter, NDF2 and coupled on to a multimode fiber, using a fiber couple (combination of objective and XY translator). The beam out from the fiber passed through a collimating lens, L1 (LA1951, Thorlabs) and then passed through a conical lens, Con.L (angle-130º) to provide a ring-shaped beam. The ring shaped beam was allowed to focus weakly onto the subject using a home made optical condenser, OC (70º, 110º) having a 50 MHz ultrasonic transducer, UST (V214-BB-RM, Olympus-NDT) in the center. An acoustic lens, AL (LC4573, Thorlabs) was attached to the bottom of the transducer which provided an acoustic focal diameter of ~46 µm. In an optically clear medium, the optical focus was around 2 mm in diameter, much wider than the ultrasonic focus. The laser repetition rate (LRR) was set to be 1 kHz and the laser energy at focus can be varied up to 30 µJ per pulse. The optical illumination on the object surface was donut shaped with a dark center so that no strong photoacoustic signals were produced from the sample surface.

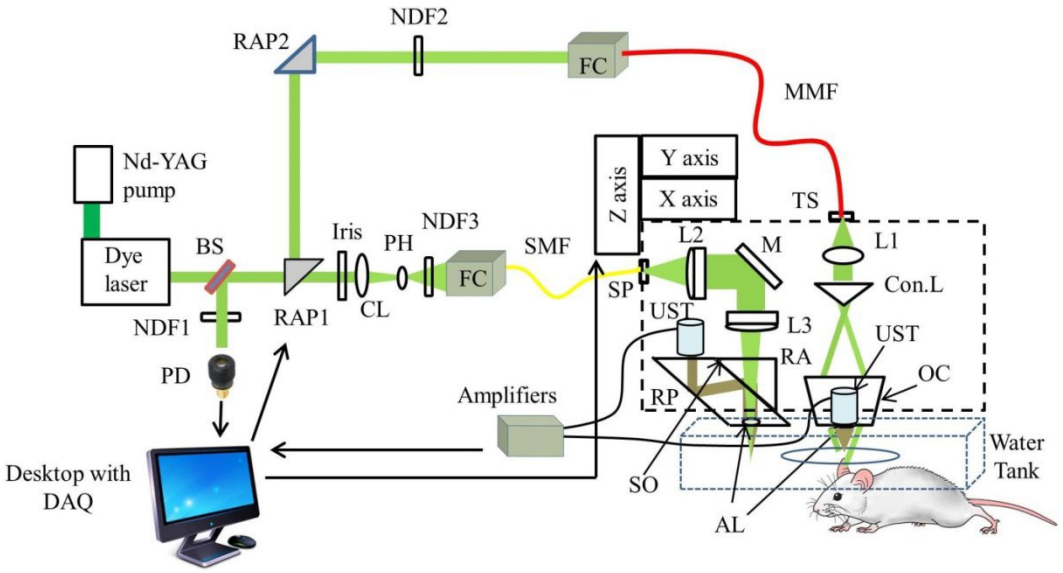


Fig. 1. (a) Schematic of the OR-AR-PAM imaging system. BS - Beam Sampler, NDF- Neutral density filter, RAP- Right angle prism, PD - photodiode, CL - Condenser lens, PH - Pinhole, FC - Fiber coupler, UST - Ultrasound transducer, MMF - Multimode fiber, SMF - Single mode fiber, DAQ - Data acquisition card, TS - Translation stage, Con.L - Conical lens, L1 - convex lens, L2&L3 - Achromatic lens, RA - Right angle prism, RP - Rhomboid prism, OC- Optical condenser, M - Mirror, SP - Slip plate, LT - Lens tube, AL - Acoustic lens.

For the OR-PAM setup the RAP1 will be rotated using the computer controlled stage so that the laser beam went straight and was reshaped by an iris and then focused by a condenser lens, CL (LA4327, Thorlabs) and passed through a pinhole, PH (P50S, Thorlabs). The filtered beam was attenuated by a variable neutral density filter, NDF3 and launched on to a single-mode fiber, SMF (P1-460B-FC-1, Thorlabs) using a single mode fiber coupler, FC (F-91-C1, Newport). The output port of the single-mode fiber was connected on a slip plate positioner, SP (SPT1, Thorlabs). The output beam from the SMF was then collimated by a Achromatic lens, L2 (32-317, Edmund Optics), reflected by a stationary elliptical mirror, M and filled the back aperture of another identical Achromatic lens, L3. The effective clear numerical aperture (NA) of the achromatic lens was 0.11. The beam then passed through a optoacoustic beam combiner consisting of a right angled prism, RA (PS615, Thorlabs) and a rhomboid prism, RP (47-214, Edmund optics) with a layer of silicon oil, SO (DMPS1M, Sigma Aldrich) in between. Similar optoacoustic beam combiner has been used earlier.[18] The silicon oil layer acts as optically transparent and acoustically reflective film. An acoustic lens, AL (LC4573, Thorlabs) provided acoustic focusing (focal diameter ~46 µm) was attached at the bottom of the rhomboid prism.. The laser repetition rate for the OR-

PAM was set to 5 kHz and the laser energy at focus can be varied up to 200 nJ per pulse. Both OR and AR systems components were also integrated and assembled in an optical cage setup.

The OR-AR combined system was attached to a home made plate for sliding the scanhead on top of the imaging area, switching between AR and OR. However, by using a y-axis translation stage with 10 cm range, manual transition can be avoided. The combined OR-AR scanner head was attached to a 3-axis motorized stage (PLS 85 for X and Y axis, VT 80 for Z axis, PI – Physik Instrumente). All the 3 stages were controlled by a 3-axis controller (SMC corvus eco, PI micos) connected to the computer. The PA signal acquired by the UST was amplified by two amplifiers (ZFL-500LN, Mini Circuits) each having 24 dB gain, and was recorded using a data acquisition card, DAQ (M4i.4420, Spectrum) in a desktop computer. The synchronization of the data acquisition and the stage motion was controlled through the signal from a photodiode, PD (SM05PD1A, Thorlabs). A beamsampler, BS (BF10-A, Thorlabs) was placed in front of the laser beam diverted a small portion of the beam (5%) to the PD. A neutral density filter, NDF 1 (NDC-50C-4M, thorlabs) was placed in front of the PD to control the energy falling on the PD. The PD signal was also used for compensating pulse to pulse variations during data acquisition. All experiments were done at a laser wavelength of 570 nm in this work.

For photoacoustic imaging the bottom of the OR-AR-PAM scanner head was submerged in a water-filled tank for acoustic coupling. A 7 cm x 7 cm area was opened in the bottom of the tank and sealed with a polyethylene membrane for optical and acoustic transmission. Two-dimensional continuous raster scanning of the imaging head was used for data acquisition. The time-resolved PA signal multiplied by speed of sound (1540 m/s) will obtain an A-line. Multiple A-lines were captured during the continuous motion of the Y stage will produce the 2 dimensional B-scan. Multiple B-scans of the imaging area were captured and stored in the computer. MATLAB was used to process and get the maximum amplitude projection (MAP) photoacoustic images.

## 3. EXPERIMENTAL RESULTS

In order to evaluate the system performance of the combined OR-AR-PAM system, a series of experiments were conducted to determine the spatial resolution, and maximum imaging depths for both AR and OR PAM.

### 3.1 LATERAL RESOLUTION OF THE IMAGING SYSTEM

The lateral resolution of the OR and AR system was determined using the sharp edge of a resolution test target. To determine the resolution of the OR-PAM system the sharp edge of a USAF resolution test target was scanned with a step size of 0.5 microns as shown in Fig. 2(a). The edge spread function (ESF) was fitted using the maximum amplitude projection (MAP) data across the edge (Fig. 2a). The line spread function (LSF) was obtained by taking the first derivative of the ESF. The full width at half maximum (FWHM) of the LSF was considered as the lateral resolution. The measured lateral resolution was 3.9 µm as shown in Fig. 2(a). Similarly the sharp edge of a USAF resolution test target was scanned with a step size of 5 microns in order to find the resolution of the AR-PAM system shown in Fig. 2(b). The measured lateral resolution was 57 µm determined from the LSF.

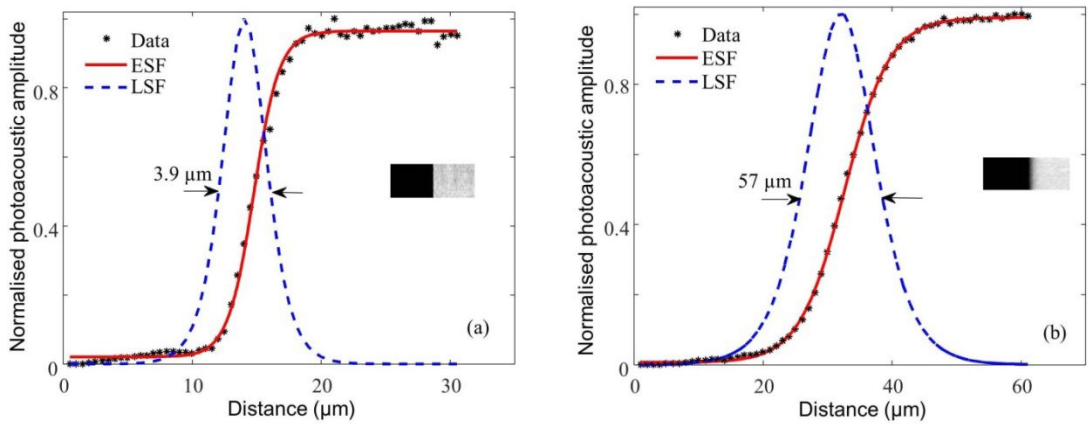


Fig. 2. Spatial resolution test of the OR-AR-PAM system: Measurement of the line spread function (LSF) using the edge of an USAF resolution target. Black (*) dots: photoacoustic signal; red line: edge spread function (ESF); blue line: line spread function (LSF): first-order derivative of the ESF for (a) OR-PAM (b) AR-PAM

### 3.2 IMAGING DEPTH

To determine the maximum imaging depth a black tape was obliquely inserted on chicken tissue as shown in Fig. 3(a). Fig. 3(b) shows the B-scan PA image. It is evident that the OR-PAM system can clearly image the black tape down to ~1.4 mm beneath the tissue surface. Similarly, using the AR-PAM system we can clearly image the black tape down to ~7.6 mm beneath the tissue surface shown in Fig.3(c). The signal-to-noise ratio (SNR) is defined as V/n, where V is the peak-to-peak PA signal amplitude, and n is the standard deviation of the background noise. For OR-PAM the SNR of the target object (black tape) at 1.4 mm imaging depth was 1.5. In case of AR-PAM the SNR at 4.6 mm and 7.6 mm imaging depth were 2.5 and 1.4, respectively.

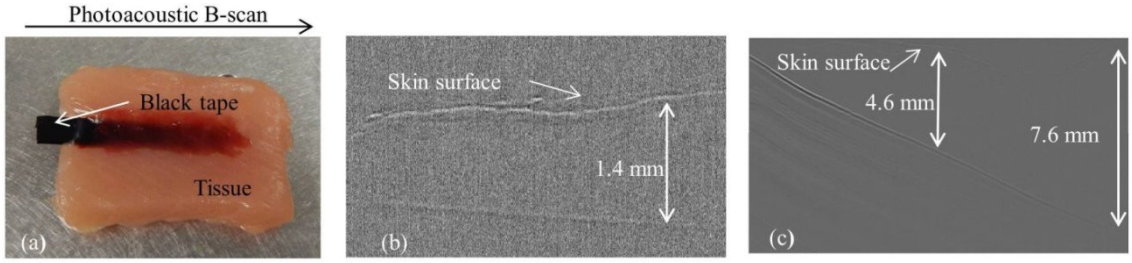


Fig. 3. Single B-scan PA image of a black tape inserted obliquely in a chicken tissue (a) Schematic diagram, (b) OR-PAM image, (c) AR-PAM image.

### 3.3 *IN VIVO* IMAGING OF MOUSE EAR BLOOD VASCULATURE

To demonstrate *in vivo* imaging using the combined system, the ear of a female mice of body weight 25 g and age 4 weeks, procured from InVivos Pte. Ltd. Singapore, were used. Animal experiments were performed according to the approved guidelines and regulations by the institutional Animal Care and Use committee of Nanyang Technological University, Singapore (Animal Protocol Number ARF-SBS/NIE-A0263). The animals were anesthetized using a cocktail of Ketamine (120 mg/kg) and Xylazine (16 mg/kg) injected intraperitoneally (dosage of 0.1 ml/10 gm). After removing hair from the ear the mouse was positioned in a platform which also has a miniature plate to position the ear. The animal was further anesthetized with vaporized isoflurane system (1 L/min oxygen and 0.75% isoflurane) during the imaging period. The imaging region was made in contact with the polyethylene membrane using ultrasound gel.

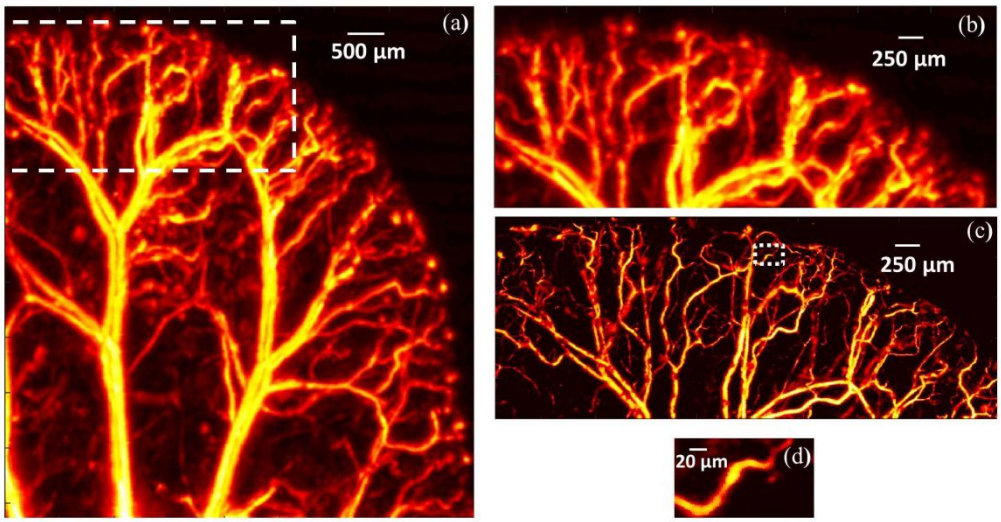


Fig. 4. *In vivo* photoacoustic image of mouse ear: (a) AR-PAM image, (b) Close up of the region of interest (ROI) in (b) as shown by white dash line, (c) OR-PAM image; (d) close up image of the ROI white dotted line in (c) showing single capillary.

Using AR-PAM an area (6.5 mm×7 mm) of the ear was first imaged, using a step size of 15 μm in the Y direction and 15 μm in the X direction. A unidirectional bscan imaging took 16 minutes to complete the AR imaging. MAP image of AR-PAM is show in Fig. 4(a). The close up of the region of interest in Fig. 4(a) is shown in Fig. 4(b). The region of interest (5 mm×2 mm), was scanned using OR-PAM with step size of 2 μm in the Y direction and 2 μm in the X direction (imaging time 42 minutes). The MAP image of the OR-PAM is shown in Fig. 4(c). The close up of the ROI in Fig. 4(c) is shown in Fig 4(d). Fig. 4(d) shows a single capillary around 10 μm diameter.

In summary an integrated OR-AR-PAM system which can achieve high resolution imaging utilizing optical focusing as well as deep tissue imaging using acoustic focusing is developed. This integrated photoacoustic microscopy system which can provide high temporal as well as spatial resolution makes the system important for applications including imaging of angiogenesis, drug response etc., where imaging single capillaries as well as deep vasculatures will be important. Further improvement in the system can be done by replacing the switchable plate with a 10 cm travelling motorized stage (y-axis). Wavefront aberration corrections for the OR-PAM will improve the lateral resolution further. Delivering higher pulse energy to the AR-PAM will improve the SNR and imaging depths as well.

## 4. CONCLUSIONS

An integrated Optical resolution and Acoustic resolution switchable photoacoustic microscopy system which can achieve both high resolution imaging at lower imaging depth and lower resolution imaging at higher imaging depth is developed. This is the first combined system using same laser which can be easily switched between OR-PAM and dark field AR-PAM. The combined system will have 3.9 μm resolution with 1.4 mm imaging depth as well as 57 μm with 7.6 mm imaging depth. The system is made of minimal home made components, making it easier to assemble, align, and build. Using the combined system *in vivo* imaging was successfully demonstrated. The developed system can be used for pre-clinical imaging. Major preclinical applications include imaging of angiogenesis, microcirculation, tumor microenvironments, drug response, brain functions, biomarkers, and gene activities.

## ACKNOWLEDGEMENT

The authors would also like to acknowledge the financial support from Tier 2 grant funded by the Ministry of Education in Singapore (ARC2/15: M4020238). Authors would like to thank Mr. Chow Wai Hoong Bobby for machine shop help. The authors would also like to thank Dr. Lidai Wang (City University of Hong Kong), Dr. Liang Song (Shenzhen Institute of Advanced Technology, Chinese Academy of Science), Dr. Junjie Yao (Duke University), and Dr. Song Hu (University of Virginia) for useful discussions. Authors have no relevant financial interests in the manuscript and no other potential conflicts of interest to disclose.

## REFERENCES

[1] Upputuri, P. K., Lin, J., Gong, L. *et al.*, "Circularly polarized coherent anti-Stokes Raman scattering microscopy," Optics Letters, 38(8), 1262-64 (2013).
[2] Upputuri, P. K., Wen, Z.-B., Wu, Z. *et al.*, "Super-resolution photoacoustic microscopy using photonic nanojets: a simulation study," Journal of Biomedical Optics, 19(11), 116003 (2014).
[3] Hu S, W. L. V., "Photoacoustic imaging and characterization of the microvasculature," Journal of Biomedical Optics, 15, (2010).
[4] Ntziachristos, V., "Going deeper than microscopy: the optical imaging frontier in biology," Nature Methods, 7(8), 603-14 (2010).
[5] Wang, L. V., and Yao, J., "A practical guide to photoacoustic tomography in the life sciences," Nat Methods, 13(8), 627-38 (2016).
[6] Upputuri, P. K., and Pramanik, M., "Recent advances toward preclinical and clinical translation of photoacoustic tomography: a review," Journal of Biomedical Optics, 22(4), 041006 (2016).
[7] Upputuri, P. K., and Pramanik, M., "Performance characterization of low-cost, high-speed, portable pulsed laser diode photoacoustic tomography (PLD-PAT) system," Biomedical Optics Express, 6(10), 4118-29 (2015).
[8] Yao, J., and Wang, L. V., "Photoacoustic Brain Imaging: from Microscopic to Macroscopic Scales," Neurophotonics, 1(1), (2014).
[9] Beard, P., "Biomedical photoacoustic imaging," Interface Focus, 1(4), 602-31 (2011).

[10] Pan, D., Pramanik, M., Senpan, A. *et al.*, "Molecular photoacoustic imaging of angiogenesis with integrin-targeted gold nanobeacons," FASEB J*,* 25(3), 875-82 (2011).
[11] Cai, X., Kim, C., Pramanik, M. *et al.*, "Photoacoustic tomography of foreign bodies in soft biological tissue," Journal of Biomedical Optics*,* 16(4), 046017 (2011).
[12] Pan, D., Pramanik, M., Senpan, A. *et al.*, "Near infrared photoacoustic detection of sentinel lymph nodes with gold nanobeacons," Biomaterials*,* 31(14), 4088-93 (2010).
[13] Wang, L. V., "Multiscale photoacoustic microscopy and computed tomography," Nature Photonics*,* 3(9), 503-509 (2009).
[14] Zhang, E. Z., Laufer, J. G., Pedley, R. B. *et al.*, "In vivo high-resolution 3D photoacoustic imaging of superficial vascular anatomy," Phys Med Biol*,* 54(4), 1035-46 (2009).
[15] Upputuri, P. K., Krishnan, M., and Pramanik, M., "Microsphere enabled sub-diffraction limited optical resolution photoacoustic microscopy: a simulation study," Journal of Biomedical Optics*,* 22(4), 045001 (2017).
[16] Zhang, H. F., Maslov, K., Stoica, G. *et al.*, "Functional photoacoustic microscopy for high-resolution and noninvasive in vivo imaging," Nature Biotechnology*,* 24(7), 848-51 (2006).
[17] Zhang, C., Maslov, K., Hu, S. *et al.*, "Reflection-mode submicron-resolution in vivo photoacoustic microscopy," Journal of Biomedical Optics*,* 17(2), 020501 (2012).
[18] Hu, S., Maslov, K., and Wang, L. V., "Second-generation optical-resolution photoacoustic microscopy with improved sensitivity and speed," Optics Letters*,* 36(7), 1134-36 (2011).
[19] Xing, W., Wang, L., Maslov, K. *et al.*, "Integrated optical-and acoustic-resolution photoacoustic microscopy based on an optical fiber bundle," Optics Letters*,* 38(1), 52-54 (2013).
[20] Estrada, H., Turner, J., Kneipp, M. *et al.*, "Real-time optoacoustic brain microscopy with hybrid optical and acoustic resolution," Laser Physics Letters*,* 11(4), 045601 (2014).
[21] Jeon, S., Kim, J., and Kim, C., "In vivo switchable optical- and acoustic-resolution photoacoustic microscopy." 9708, 970845.
[22] Moothanchery, M., Sharma, A., and Pramanik, M., "A Switchable Acoustic and Optical Resolution Photoacoustic Microscopy for *in vivo* small animal blood vasculature imaging," Journal of Visualized Experiments 2017 (Under Review).
[23] Moothanchery, M., and Pramanik, M., "Performance Characterization of a Switchable Acoustic and Optical Resolution Photoacoustic Microscopy,"Sensors 2017 (Under Review)